Supporting Information

Synthesis of Ag_3PO_4 Crystals with Tunable Shapes for Facet-Dependent Optical Property, Photocatalytic Activity and Electrical Conductivity Examinations

Meng-Shan Hsieh,[†] Huang-Jen Su,[‡] Pei-Lun Hsieh,[§] Yun-Wei Chiang,[†] and Michael H. Huang[*,†]

[†]Department of Chemistry, [‡]Interdisciplinary Program of Sciences, and [§]Department of Materials Science and Engineering, National Tsing Hua University, Hsinchu 30013, Taiwan

E-mail: hyhuang@mx.nthu.edu.tw

Experimental Section

Electron Paramagnetic Resonance Analysis. To detect hydroxyl radicals generated from a photocatalyst, DMPO (5,5-dimethyl-1-pyrroline N-oxide) is commonly introduced as a spin trapping agent. A 0.1 M DMPO solution was prepared by adding 67.9 mg of DMPO to 6 mL of deionized water. The 6 mL of 0.1 M DMPO solution was carefully injected through 2 mL of activated carbon solution in a syringe fitted with a 0.45 μm filter at the syringe tip. The injection was repeated two more times to ensure clean EPR spectra can be obtained. The synthesized Ag_3PO_4 cubes (732 nm), rhombic dodecahedra (362 nm), and tetrahedra (600 nm) with particle surface area ratios of 1 : 2.02 : 2.99 initially stored in ethanol were dried and weighted. 10.9, 5.4, and 3.6 mg of Ag_3PO_4 cubes, rhombic dodecahedra, and tetrahedra having the same total particle surface area (0.0882 m^2) were dispersed in 1 mL of deionized water with sonication, then 1 mL of 0.1 M DMPO was added into the solution. The solution was irradiated by a 500-W Xenon lamp with stirring for 5 min and sent for EPR analysis immediately. The EPR signals of radicals spin-trapped by DMPO were all recorded at ambient temperature. The settings of EPR instrument were: microwave frequency 9.80 GHz, microwave power 15.0 mW, sweep width 100 G, modulation frequency 100 kHz, and modulation amplitude 1 G.

Electrical Conductivity Measurements. For electrical conductivity measurements on single Ag_3PO_4 crystals, tungsten probes were prepared from tungsten wires (99.95%, Alfa Aesar). A direct current (15 V and 1.5 A) was applied to sharpen the wire tips by electrolysis in a 2.0 M NaOH solution. After finishing electrolysis in 1 min, the tungsten wire tips have reduced to ~ 300 nm. To remove the tungsten oxide layer on the wire surface, the probe tips were immersed into a 10 M KOH solution for 5 s. Separately, a Si (111) substrate was annealed at 900 ºC in air atmosphere in a tube furnace for 48 h to form a SiO_2 layer thicker than 500 nm on the substrate as an insulating layer to prevent leakage current flowing from the Ag_3PO_4 crystal to the Si substrate. Next, a dilute solution of Ag_3PO_4 crystals was dropped on the thermally treated Si substrate. After evaporating the droplet, the Si substrate with Ag_3PO_4 particles was loaded inside a JEOL 7000F scanning electron microscope. The treated tungsten probes were installed on a nanomanipulator (Kammrath & Wiess GmbH), which was connected to a Keithley Model 4200-SCS source measurement unit. The nanomanipulator was loaded inside the same electron microscope. The two tungsten probes were first brought in contact with an electric current applied until a linear $I-V$ curve was obtained. This $I-V$ curve signifies purely metallic contact has been formed and any surface oxide was removed.

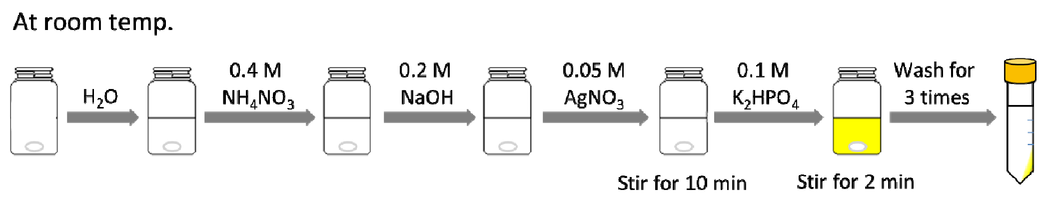

Scheme S1. Illustration of the general procedure used to make Ag_3PO_4 crystals with tunable shapes.

Table S1. Exact reagent amounts used in the growth of Ag_3PO_4 crystals with tunable shapes.

Shape	H_2O	0.4 M NH_4NO_3	0.2 M NaOH	0.05 M $AgNO_3$	0.1 M K_2HPO_4	Total volume
Cubes	8920.0 μL	100 μL	180 μL	400 μL	400 μL	10 mL
Rhombic Dodecahedra	8420.0 μL	600 μL	180 μL	400 μL	400 μL	10 mL
{100}-Truncated Rhombic Dodecahedra	8120.0 μL	600 μL	180 μL	550 μL	550 μL	10 mL
Tetrahedra	1887.4 μL	218.8 μL	393.8 μL	500 μL	0.7 M 7000 μL	10 mL
Tetrapods	1887.4 μL	281.3 μL	506.3 μL	500 μL	0.7 M 7000 μL	10 mL

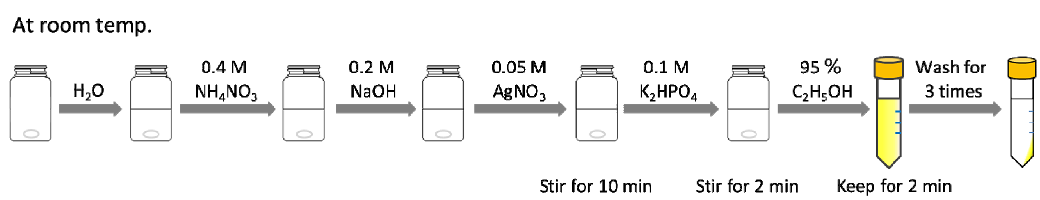

Scheme S2. Illustration of the procedure used to make smaller Ag_3PO_4 rhombic dodecahedra and tetrahedra.

Table S2. Exact reagent amounts used in the growth of smaller Ag_3PO_4 rhombic dodecahedra and tetrahedra.

Shape	H_2O	0.4 M NH_4NO_3	0.2 M NaOH	0.05 M $AgNO_3$	0.1 M K_2HPO_4	Total volume	95 % C_2H_5OH
Rhombic Dodecahedra	8495 μL	600 μL	180 μL	325 μL	400 μL	10 mL	7.5 mL
Tetrahedra	2062.4 μL	218.8 μL	393.8 μL	325 μL	0.7 M 7000 μL	10 mL	7.5 mL

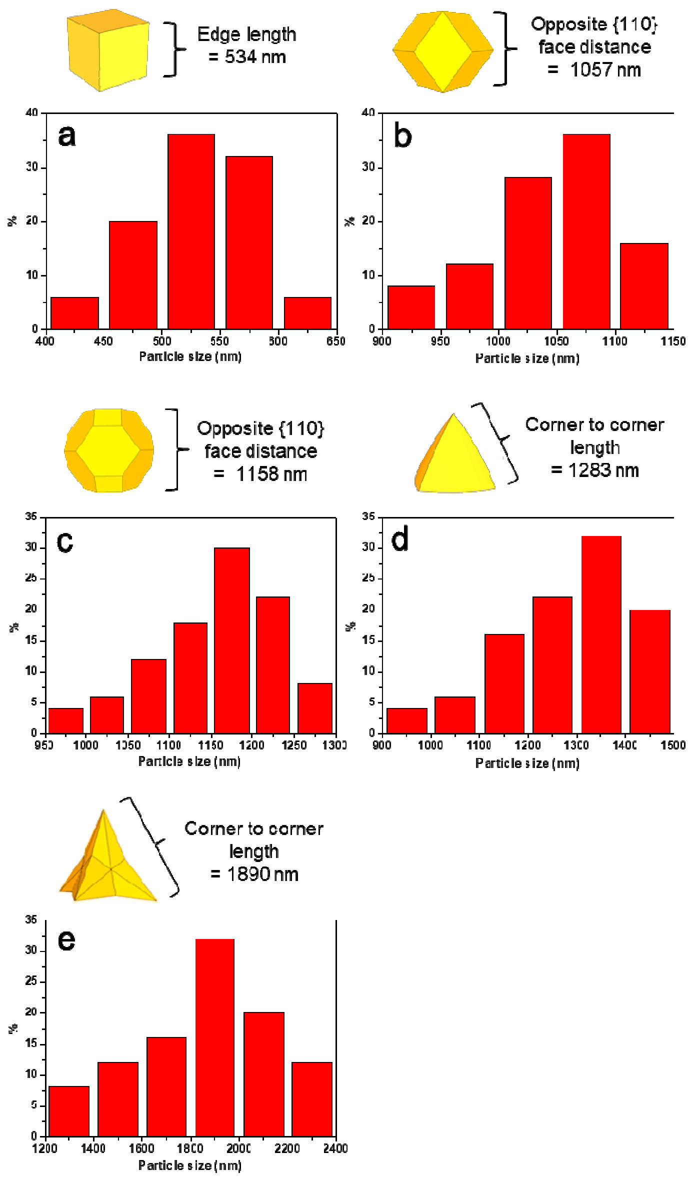

Figure S1. Size distribution histograms of Ag_3PO_4 (a) cubes, (b) rhombic dodecahedra, (c) {100}-truncated rhombic dodecahedra, (d) tetrahedra, and (e) tetrapods. The measured lengths are indicated.

Table S3. Average Ag_3PO_4 crystal sizes and their standard deviations.

Shapes	Average particle size (nm)	Standard deviation (%)
Cubes	534 ± 47	9
Rhombic Dodecahedra	1057 ± 60	6
{100}-Truncated Rhombic Dodecahedra	1158 ± 77	7
Tetrahedra	1283 ± 121	9
Tetrapods	1890 ± 269	14

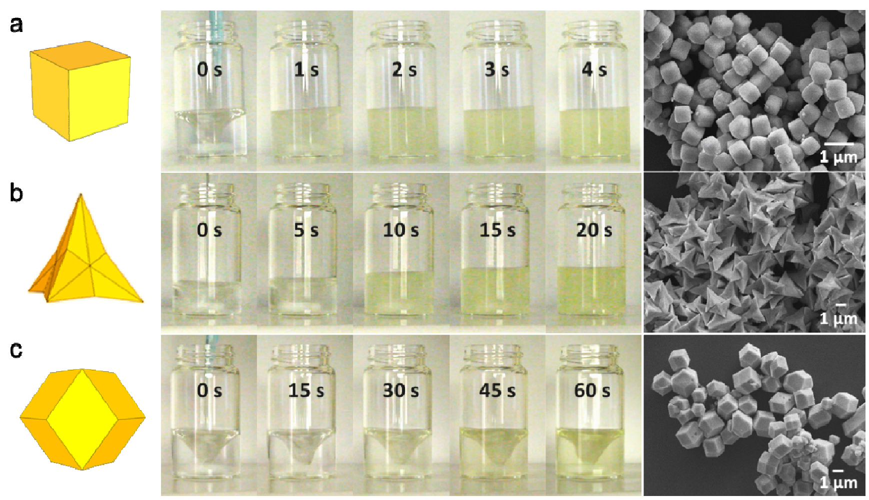

Figure S2. Photographs and SEM images showing different growth rates in the formation of Ag_3PO_4 (a) cubes, (b) tetrapods, and (c) rhombic dodecahedra through observation of their solution color changes as a function of reaction time.

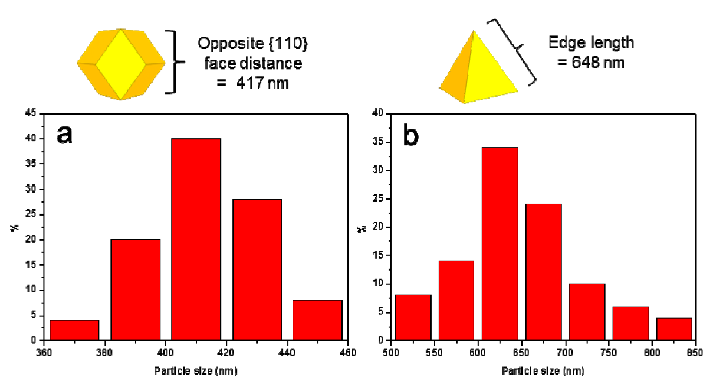

Figure S3. Size distribution histograms of smaller Ag_3PO_4 (a) rhombic dodecahedra and (b) tetrahedra. The measured lengths are indicated.

Table S4. Average sizes of the smaller Ag_3PO_4 rhombic dodecahedra and tetrahedra.

Shape	Average particle size (nm)	Standard deviation (%)
Rhombic Dodecahedra	417 ± 18	4
Tetrahedra	648 ± 76	12

Table S5. Reaction conditions and procedures used to make Ag_3PO_4 cubes and rhombic dodecahedra with tunable sizes. Ethanol was used only for preparing 298 nm rhombic dodecahedra. Due to the fast reaction, consistent control of particle sizes was not always achieved despite following the same reaction conditions.

Cubes	H_2O	0.4 M NH_4NO_3	0.2 M NaOH	0.05 M $AgNO_3$	0.1 M K_2HPO_4	Total volume
365 nm	8380 μL	150 μL	270 μL	600 μL	600 μL	10 mL
462 nm	8920 μL	100 μL	180 μL	400 μL	400 μL	10 mL
530 nm	8920 μL	100 μL	180 μL	400 μL	400 μL	10 mL
648 nm	8920 μL	100 μL	180 μL	400 μL	400 μL	10 mL

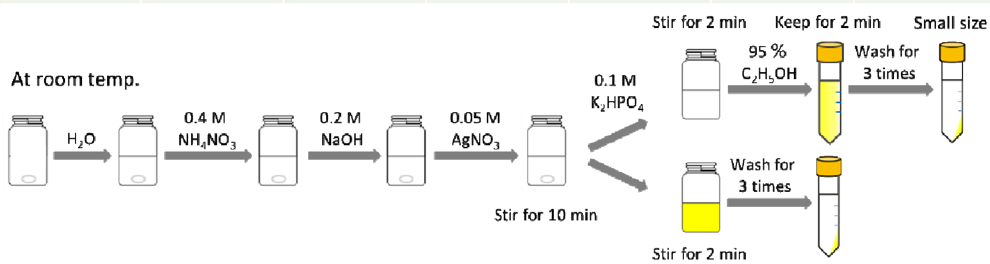

RD	H_2O	0.4 M NH_4NO_3	0.2 M NaOH	0.05 M $AgNO_3$	0.1 M K_2HPO_4	Total volume	95 % C_2H_5OH
289 nm	8495 μL	600 μL	180 μL	325 μL	600 μL	10 mL	7.5 mL
643 nm	8420 μL	600 μL	180 μL	400 μL	400 μL	10 mL	X
993 nm	8420 μL	600 μL	180 μL	400 μL	400 μL	10 mL	X
1314 nm	8420 μL	600 μL	180 μL	400 μL	400 μL	10 mL	X

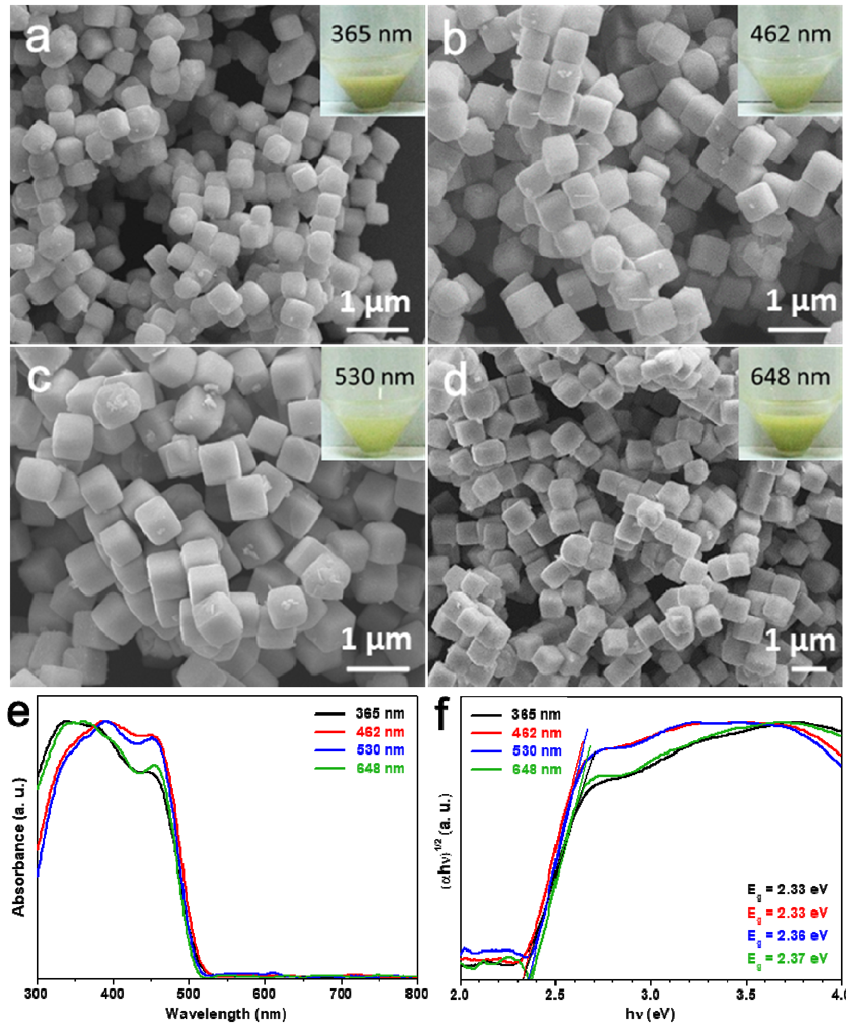

g

Size	Volume	E_g	Wavelength
365 nm	4.8 x 10^7 nm^3	2.33 eV	532 nm
462 nm	9.7 x 10^7 nm^3	2.33 eV	532 nm
530 nm	1.5 x 10^8 nm^3	2.36 eV	525 nm
648 nm	2.7 x 10^8 nm^3	2.37 eV	523 nm

Figure S4. (a–d) SEM images of Ag_3PO_4 cubes with edge lengths of (a) 365, (b) 462, (c) 530, and (d) 648 nm. Insets show their solution colors. (e) Diffuse reflectance spectra of these Ag_3PO_4 cubes. (f) Tauc plot of these Ag_3PO_4 cubes to determine their indirect optical band gaps. (g) Volumes of these cubes and their band gaps and the corresponding light wavelengths.

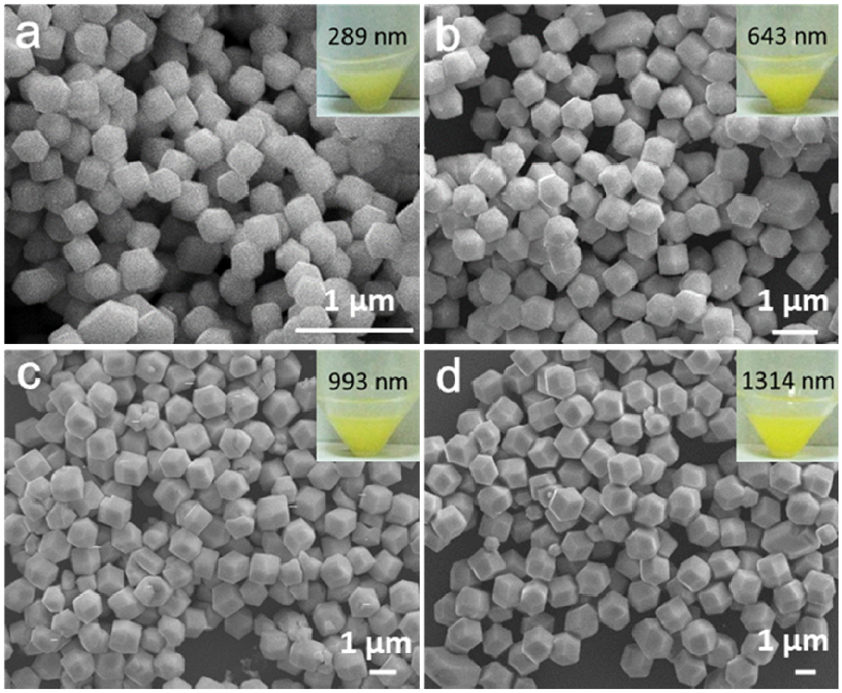

e

Size	Volume	E_g	Wavelength
289 nm	1.7×10^7 nm^3	2.25 eV	551 nm
643 nm	1.9×10^8 nm^3	2.34 eV	530 nm
993 nm	6.9×10^8 nm^3	2.34 eV	530 nm
1314 nm	1.6×10^9 nm^3	2.35 eV	528 nm

Figure S5. (a–d) SEM images of Ag_3PO_4 rhombic dodecahedra with opposite face distances of (a) 289, (b) 643, (c) 993, and (d) 1314 nm. Insets show their solution colors. (e) Volumes of these rhombic dodecahedra and their band gaps and the corresponding light wavelengths.

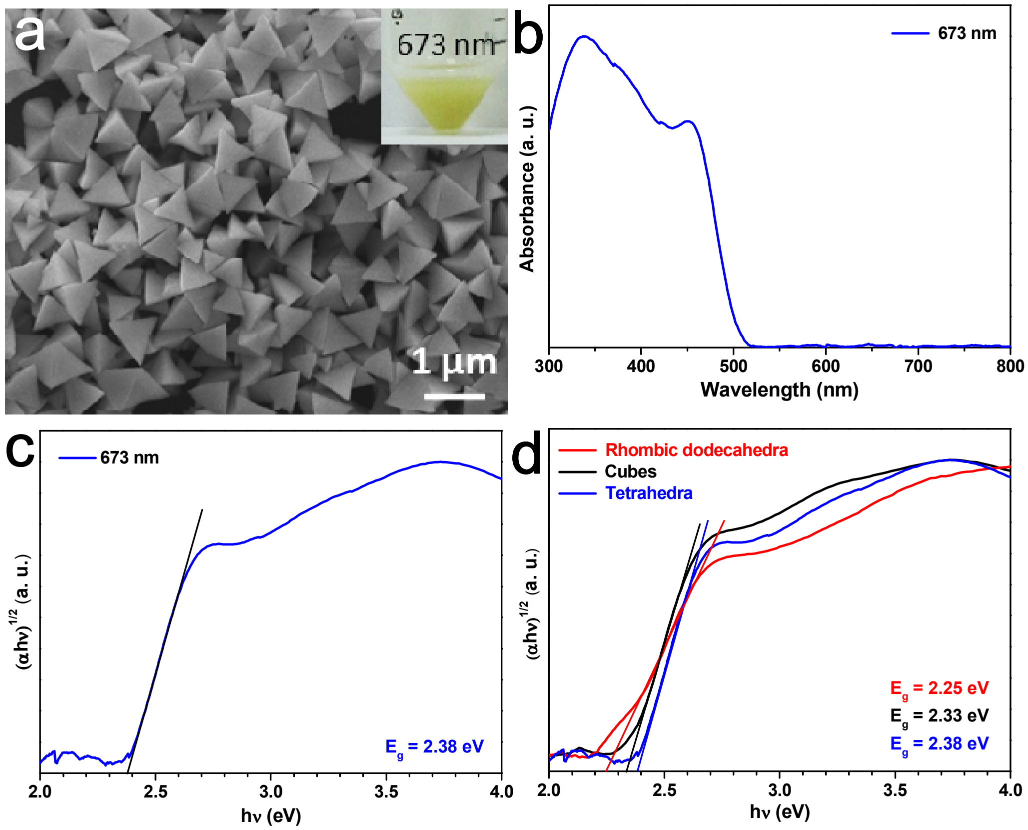

e

Shape	Size	Volume	E_g	Wavelength
Rhombic dodecahedra	289 nm	1.7×10^7 nm^3	2.25 eV	551 nm
Cubes	365 nm	4.8×10^7 nm^3	2.33 eV	532 nm
Tetrahedra	673 nm	3.6×10^7 nm^3	2.38 eV	521 nm

Figure S6. (a) SEM images of Ag_3PO_4 tetrahedra with an average edge length of 673 nm. Insets show the solution color. (b) Diffuse reflectance spectra of the Ag_3PO_4 tetrahedra. (c) Tauc plot of the Ag_3PO_4 tetrahedra to determine their indirect optical band gaps. (d) Tauc plots for Ag_3PO_4 rhombic dodecahedra, cubes, and tetrahedra having similar particle sizes for comparison of their band gap values. (e) Volumes of the particles shown in panel d and their band gaps and the corresponding light wavelengths.

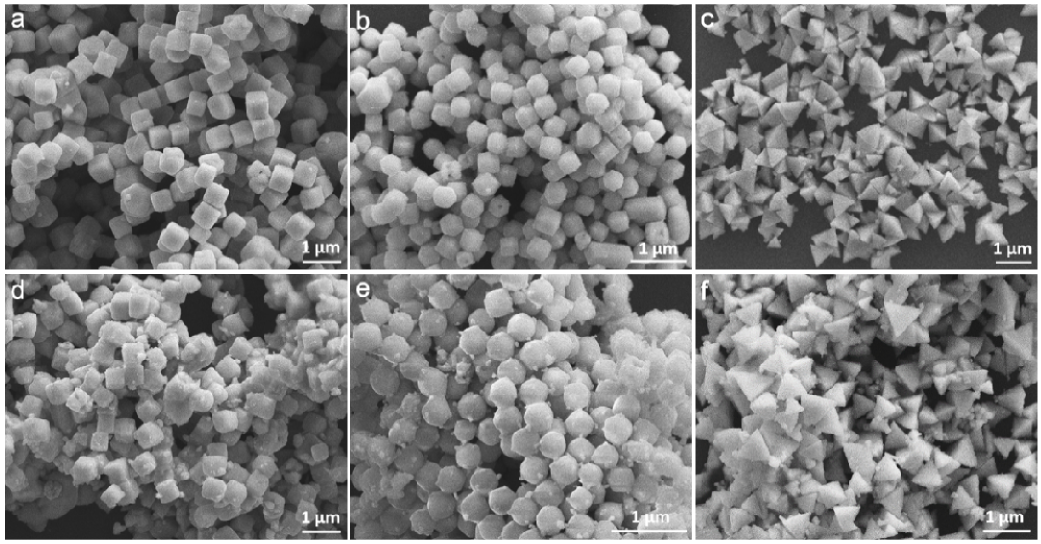

Figure S7. SEM images of Ag_3PO_4 (a, d) cubes, (b, e) rhombic dodecahedra, and (c, f) tetrahedra before (a–c) and after (d–f) 90 min of the photoirradiation experiment.

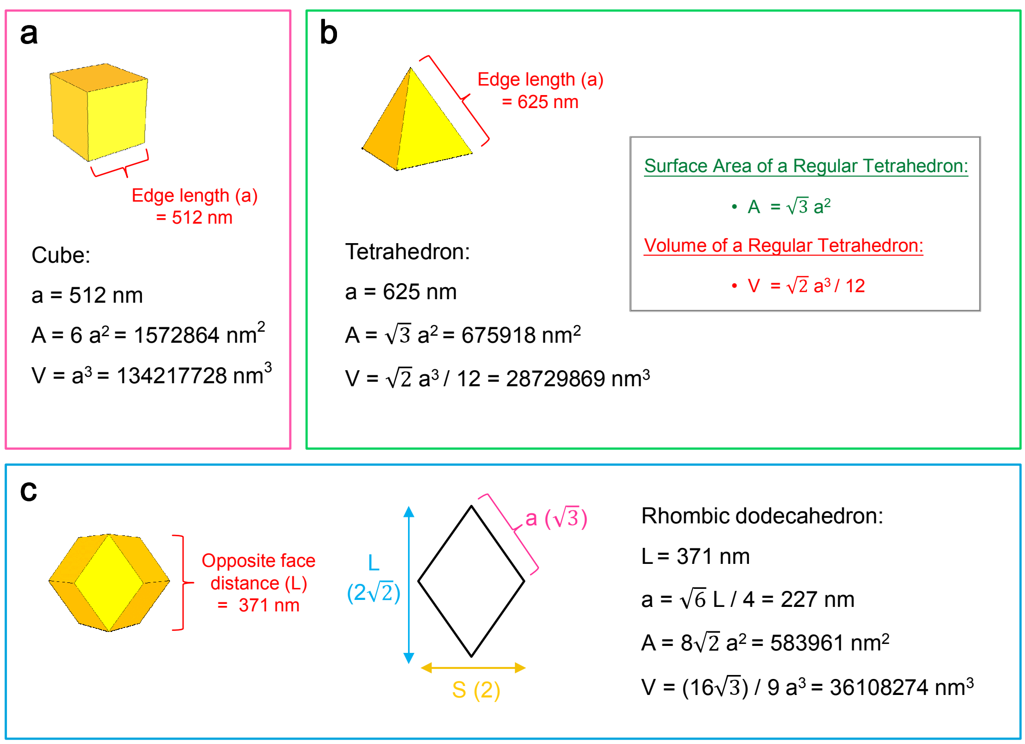

Figure S8. Calculations of the surface area and volume of a single Ag_3PO_4 (a) cube, (b) tetrahedron, and (c) rhombic dodecahedron.

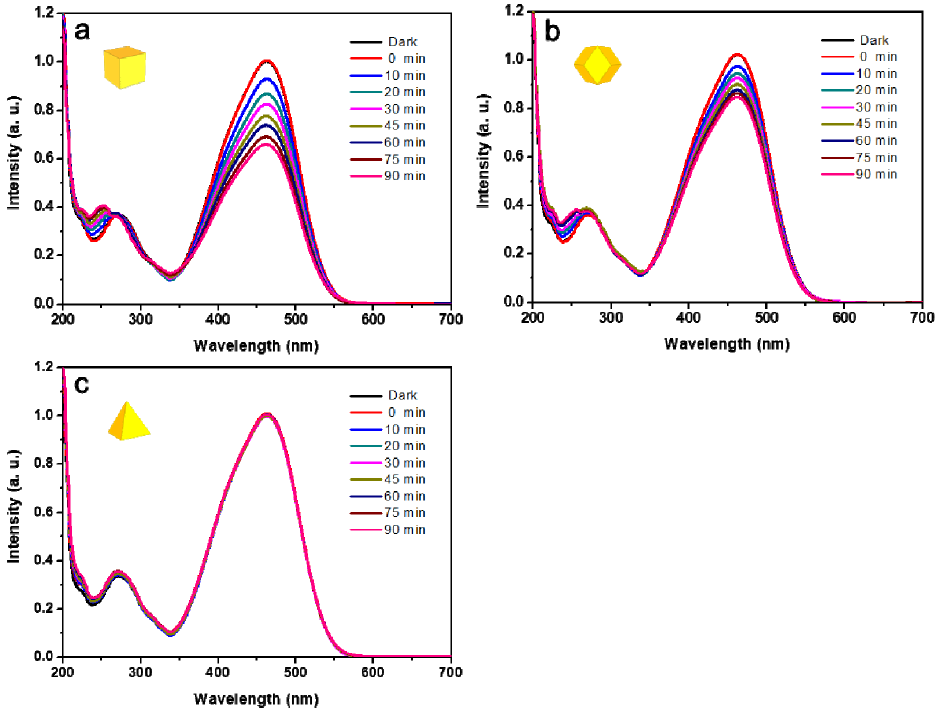

Figure S9. UV-vis absorption spectra of methyl orange as a function of irradiation time using Ag_3PO_4 (a) cubes, (b) rhombic dodecahedra, and (c) tetrahedra as the photocatalysts.

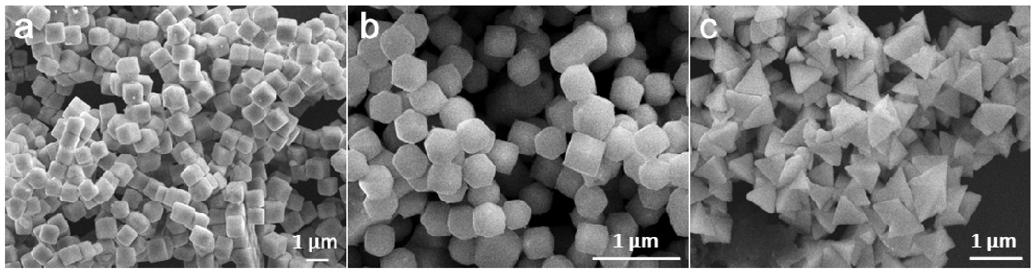

Figure S10. SEM images of Ag_3PO_4 (a) cubes, (b) rhombic dodecahedra, and (c) tetrahedra used for EPR measurements.

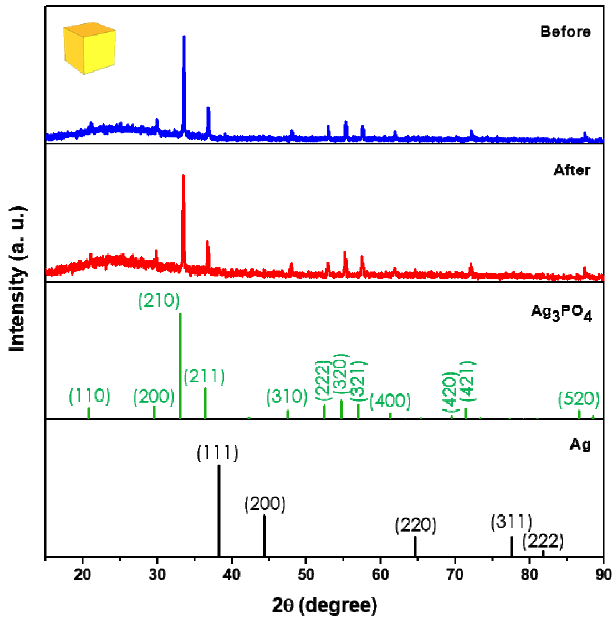

Figure S11. XRD patterns of Ag_3PO_4 cubes before and after the photocatalysis experiment. The standard patterns of Ag_3PO_4 and Ag are shown.

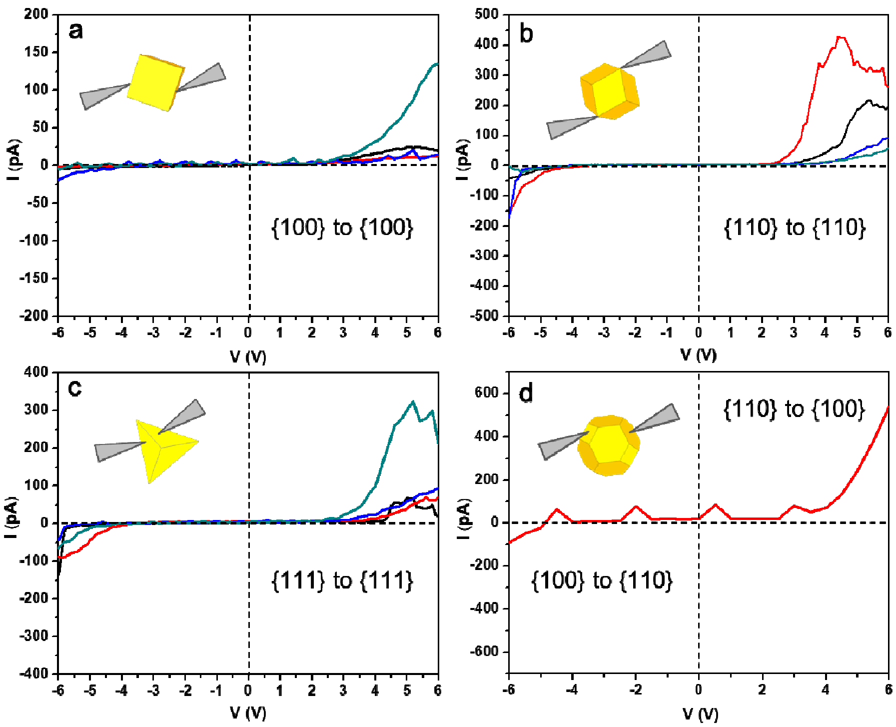

Figure S12. (a–c) Multiple I–V curves measured on a single Ag_3PO_4 (a) cube, (b) rhombic dodecahedron, and (c) tetrahedron. (d) One I–V curve obtained with W probes contacting the {110} and {100} faces of a Ag_3PO_4 {100}-truncated rhombic dodecahedron.